Jacob Mims & Mohamed Laradji

Self-Induced Spatial Organization of Nanoparticles in a Polymer Brush: A Molecular Dynamics Study

Faculty Sponsor

Dr. Mohamed Laradji

Abstract

The interactions of spherical nanoparticles absorbed into a polymer brush was investigated using molecular dynamics simulations of a coarse-grained implicit solvent model. Our simulations indicate a few phenomenon including self-assembly into superstructures that contain HCP and FCC symmetries.

Introduction

Understanding the way nanoparticles (NPs) interact with various media can lead the way to the development of advanced materials. One such important media would be a polymer brush. This understanding is important for the development of lightweight nanomaterials for use in the automobile and aerospace industries. It would also give further insight into biomedical applications, which can help deter potential toxic effects on living organisms. One such important phenomenon would be self-assembly of the nanoparticles.

Interactions between NPs and polymer brushes have been studied both theoretically and experimentally for differing applications. Kim *et al.* performed self-consistent field theory calculations to study the repulsive effect of polymer brushes cushioning a single NP.[1] Kesal *et al.* used an experimental set-up to study the attractive interactions between gold NPs and a polyelectrolyte brush.[2] The varying attempts to characterize such interactions shows the interest in these types of problems.

Recently in our group, studies have been conducted on NPs at the interface of a lipid membrane.[3, 4] In these studies, certain self-assembled structures were found, and their stability was characterized. There have also been Molecular Dynamics simulations in the case of spatial organization in polymer brushes. Cheng *et al*. investigated a system in which NPs are placed randomly above a brush in an evaporating solvent.[5] After evaporation, a neatly organized layer could be seen.

Some experimental studies have shown that the interactions between NPs and various polymer medias can lead to spatial organization. Bockstaller *et al*. used diblock copolymers to induce spatial organization in the NPs in their system.[6] In order to further probe interactions between NPs and polymer brushes, a series of systematic Molecular Dynamics simulations were conducted.

Model and Computational Method

In this study, we used a coarse-grained implicit-solvent model that was developed to study self-assembled lipid membranes.[7, 8] This model has been adapted to describe fully flexible linear homopolymer chains for use in these simulations, coarse-graining the chain into many monomers. The potential energy of the polymer chains is comprises two contributions:

$$U(\{\vec{r_i}\}) = \sum_{i,j} U_0^{\alpha_i \beta_j}(r_{ij}) + \sum_{<i,j>} U_{\text{bond}}(r_{ij}) \qquad (1)$$

where $\vec{r}_i$ describes the coordinates for the center of mass for particle *i* in the simulation, $r_{ij} = |\vec{r}_i - \vec{r}_j|$, and α_i indicates the type of particle that *i* is, i.e. $\alpha_i = m$ for a monomer or $\alpha_i = s$ for an NP. In the second contribution of Eq. 1, the angled brackets indicate that *i* and *j* are constituents of the same polymer chain. $U_0^{\alpha\beta}$ is a soft two-body potential between two particles of types α and β that are separated by some distance *r*, given by a piece-wise function:

$$U_0^{\alpha\beta}(r) = \begin{cases} \left(U_{\max}^{\alpha\beta} - U_{\min}^{\alpha\beta}\right)\dfrac{(r_m - r)^2}{r_m^2} + U_{\min}^{\alpha\beta} & \text{if } r \le r_m, \\ 0 & \text{if } r > r_m, \end{cases} \tag{2}$$

where $U_{\max}^{\alpha\beta} > 0$ and $U_{\min}^{\alpha\beta} \le 0$ for any pairing of (α, β). For monomers, this piecewise potential implies a repulsive force up to r_m, which is half of the radial cutoff, r_c.

In Eq. 1, the second term, $U_{\text{bond}}(r_{ij})$, is a harmonic potential used to ensure the connectivity of monomers along the same polymer chain. Explicitly:

$$U_{\text{bond}}(r) = \frac{k_{\text{bond}}}{2}(r - a_b)^2 \tag{3}$$

Wherein, k_{bond} is the bond stiffness coefficient and a_b is the preferred bond length. It is also important to note that bonded monomers interact with each other with Eq. 2 along with Eq. 3.

In our model, NPs are assumed to be a sphere of radius R and a homogenous surface. Under this assumption, NPs are sufficiently described with only three degrees of freedom, each of which correspond to the center of mass of the NP. This is due to the spherical symmetry of the NP. This is in stark contrast to the numerous degrees of freedom that are implied by a model that constructs NPs by beads connected by fluctuating bonds.[9] The interaction that occurs among a monomer and an element of the NP's surface area, δ*a*, separated by some distance ρ is assumed to have the same form as Eq. 2, but has an added condition that allows for an attractive force between a monomer and the NP. Explicitly stated,

$$\delta U^{s\alpha}(r) = \begin{cases} \left[(u_{\max}^{s\alpha} - u_{\min}^{s\alpha})\dfrac{(r_m - \rho)^2}{r_m^2} + u_{\min}^{s\alpha}\right]\delta a & \text{if } \rho \le r_m, \\ \left[-2u_{\min}^{s\alpha}\dfrac{(r_c - \rho)^3}{(r_c - r_m)^3} + 3u_{\max}^{s\alpha}\dfrac{(r_c - \rho)^2}{(r_c - r_m)^2}\right]\delta a & \text{if } r_m < \rho \le r_c, \\ 0 & \text{if } \rho > r_c, \end{cases} \tag{4}$$

where $u_{\min}^{s\alpha}$ is the value of the potential, per unit of area, that is separated some distance r_m from the surface of the NP. Due to the fact that this is a soft potential, the inequality $u_{\max}^{s\alpha} > 0$ is required and the value of the parameter must be strong enough to prevent monomers from penetrating into the NP. $u_{\min}^{s\alpha} = 0$ implies a fully repulsive interaction between a NP and another particle of type α, and $u_{\min}^{s\alpha} < 0$ implies a short-range attractive interaction. The total interaction between an NP and some particle of type α, $U^{sa}(r)$, is given by integrating Eq. 4 over the surface of the NP and explicitly given by

$$U^{s\alpha}(r) = \begin{cases} 2\pi r_m^2 \frac{R}{r}\left[\frac{A^{s\alpha}(R+r_m-r)^4}{4r_m^4} - \frac{A^{s\alpha}(R+r_m-r)^3}{3r_m^3} - \frac{u_{\min}^{s\alpha}(R+r_m-r)^2}{2r_m^2} + \frac{u_{\min}^{s\alpha}(R+r_m-r)}{r_m} + \frac{13u_{\min}^{s\alpha}}{20}\right] & \text{if } r \le R + r_m \\ 2\pi r_m^2 \frac{R}{r}\left[\frac{2u_{\min}^{s\alpha}(R+r_c-r)^5}{5r_m^5} - \frac{7u_{\min}^{s\alpha}(R+r_c-r)^4}{4r_m^4} + \frac{2u_{\min}^{s\alpha}(R+r_c-r)^3}{r_m^3}\right] & \text{if } R + r_m < r \le R + r_c \\ 0 & \text{if } r > R + r_c \end{cases} \quad (5)$$

where $A^{s\alpha} = u_{\min}^{s\alpha} - u_{\max}^{s\alpha}$.

All monomers and NPs' center of mass are moved using a molecular dynamics scheme with a Langevin thermostat, i.e.

$$\dot{r}_i(t) = v_i(t), \quad (6)$$

$$m_i \dot{v}_i(t) = -\nabla U(\{r_i\}) - \Gamma v_i(t) + \sigma \Xi_i(t) \quad (7)$$

where m_i is the mass of particle i and Γ is a particle's drag coefficient. $\sigma\Xi_i(t)$ is a random force with zero that is uncorrelated for differing particles and times. Γ and σ are inter-related through the fluctuation–dissipation theorem, leading to the equality $\Gamma = \sigma^2 / 2k_b T$.

For our simulations, the model's parameters are given by the following:

$$\begin{gathered} U_{\min}^{mm} = 0 \\ U_{\max}^{mm} = 100\epsilon \\ u_{\min}^{sm} = 0 \\ u_{\max}^{sm} = 235.2\epsilon / r_m^2 \\ u_{\max}^{ss} = 235.2\epsilon / r_m^2 \\ k_{\text{bond}} = 100\epsilon / r_m^2 \\ a_b = 0.7 r_m \end{gathered} \quad (8)$$

For all the simulations in this study, they were performed at $k_b T = 3.0$ with a time step of $\Delta t = 0.02\ \tau$. Eqs. 1 and 2 are integrated using a standard velocity-Verlet method where $\Gamma = \sqrt{6m/\tau}$[10].

For this study, we consider a case where varying numbers of NPs with diameter $D_{np} = 4R$ are placed randomly above a polymer brush. This polymer brush is consisted of a set number of chains $N_{chains} = 800$ and each chain consists of 100 monomers. The chains have been grafted randomly onto a static substrate using a metropolis Monte-Carlo Method. The area

of the xy-plane of the simulation box is determined with the parameters of this grafting, being $\text{Area}_{xy} = N_{chains}$ /σ where σ is the grafting density of polymers.σ The polymer chains remain grafted throughout the simulation by not time-evolving the monomers that are used to graft the chains. The simulation box extends into the z axis to give enough room for the NPs to be placed without overlapping.

Results and Discussion

Fig. 1 contains snapshots of various systems at an equilibrated state with the corresponding value of $|U_{min}|$ labeled providing a nice qualitative overview of the study. As shown in the figure, NPs begin penetrating the brush at low values of $|U_{min}|$ and the fraction absorbed increases along with said parameter. For the case of this system, the NPs are fully absorbed into the brush at $|U_{min}| = 0.3$. These absorbed NPs then find their way deeper into the brush with increasing $|U_{min}|$. Saliently, the snapshot at $|U_{min}| = 0.3$ showcases the NPs ability to self-assemble into a well-ordered superstructure with next to no diffusivity. At lower values, the NPs penetrate the brush and are dispersed into a liquid-type state with no order. The NPs in this liquid-type state retain some value of diffusivity. As the value of $|U_{min}|$ increases from the form that needed for a superstructure, the NPs form an amorphous glass with almost no diffusivity.

In Figs. 2 and 3, there is a clear dependence of the average height of the

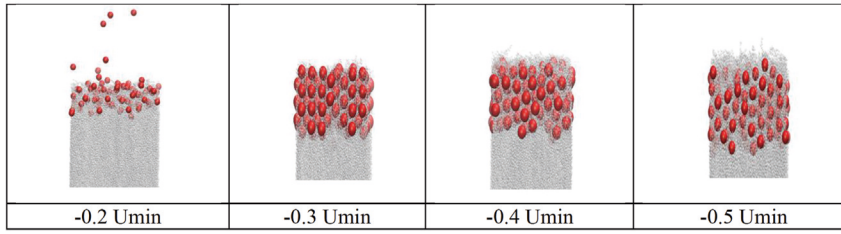

Figure 1. Side-view snapshots taken from different systems of 800 Chains 224 NPs and 0.5 grafting density.

NPs on the value of $|U_{min}|$ In both graphs, there is an initial stark downwards trend that begins to saturate and level off. This saturation is prescribed by the polymer brush. As the NPs continually dive deeper into the brush, they eventually reach a point at which the value of the monomer density is too high to permit them to reach further into it. The monomer density is proportional to the grafting density of the polymer brush. This would explain how the NPs at a lower value of grafting density would have a lower minimum height.

In Fig. 3, the average height of the NPs inhabiting the less-dense brush begins to level off at $|U_{min}|= 0.2$, while their higher density counterparts start at $|U_{min}|= 0.3$. This implies that, as the grafting density of the polymer brush is lowered, the threshold value of $|U_{min}|$ for the NPs to be penetrative is decreased.

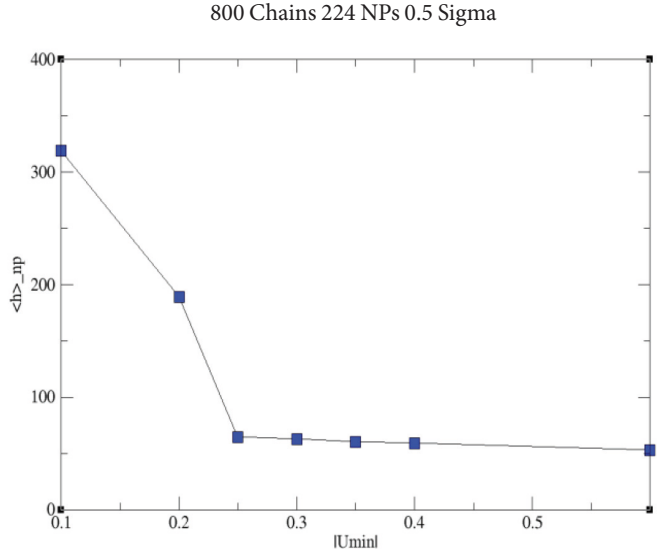

Figure 2. Average height of the NPs as a function of $|U_{min}|$. This data was taken from a system of 800 chains, 224 NPs, and grafting density of

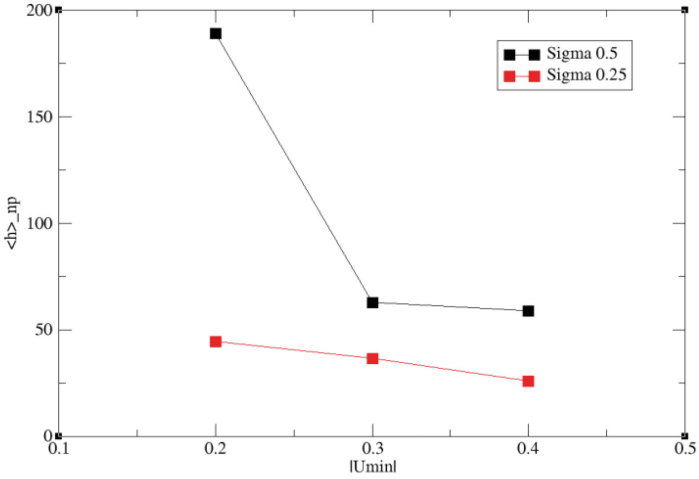

Figure 3. Average height of the NPs as a function of $|U_{min}|$. This data was taken from systems with 800 chains, 224 NPs, and variable grafting densities. his data was taken from a system of 800 chains, 224 NPs, and grafting density of 0.5

In Figs. 4, 5 and 6 the lefthand column shows of density profiles along the z-axis for three varying systems at an equilibrated state, while the right hand column is shows a corresponding snapshot. These snapshots showcase the three different states penetrative NPs. The upper-most row (Figure 6) showcases the liquid-type state, in which the NPs still show some manner of diffusivity. The NPs in this state showcase no order and inhabit a shallow location. The next row (Figure 5) showcases a system of great crystalline order, with the oscillatory NP and polymer profiles being characteristic of this order. Although these oscillatory profiles greatly characterize order, they fail to define a specific orientation. As of now, it appears as though the crystalline structures can take any number of preferred orientations inside of the brush. The bottom-most row (Figure 4) provides an example of an amorphous solid formed by the NPs. In terms of $|U_{min}|$, penetrative NPs enter and take a liquid-type configuration and with increasing $|U_{min}|$ the NPs will find a range of great order and then melt into an amorphous solid.

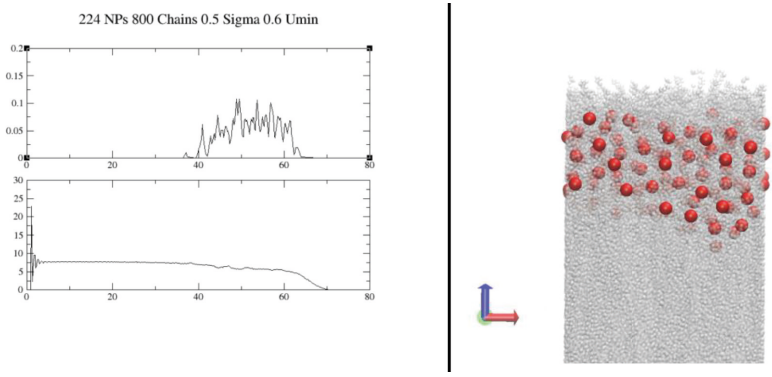

Figure 4. $|U_{min}|$ 0.6 Density profile of NPs & monomers (left) and snapshot of system (right)

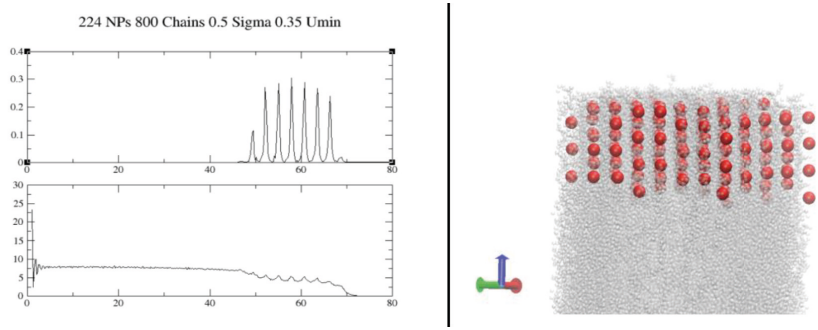

Figure 5. $|U_{min}|$ 0.35 Density profile of NPs & monomers (left) and snapshot of system (right)

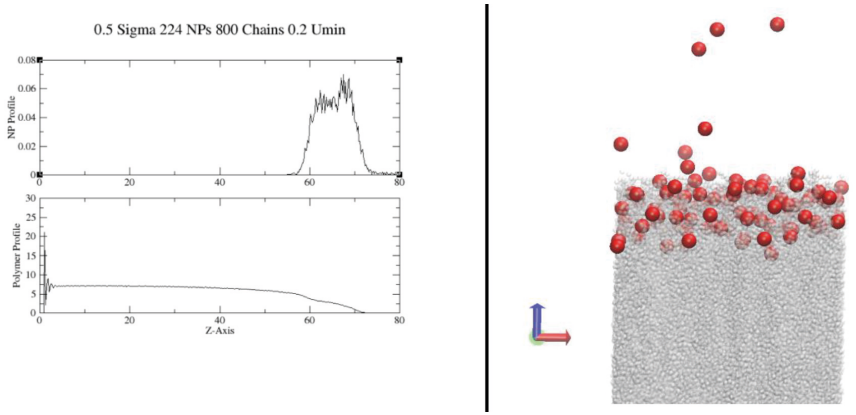

Figure 6. $|U_{min}|$ 0.2 Density profile of NPs & monomers (left) and snapshot of system (right)

The radial distribution function (rdf) of NPs in a crystalline configuration is plotted in Fig. 7. This rdf has peaks that are characteristic of both HCP and FCC crystals. HCP and FCC unit cells were observed in said simulation and snapshots are provided in Fig. 8. Both unit cells are commonly found inside naturally formed lattices; a FCC unit cell can be made into a HCP by rotating the third layer (the most transparent layer) of the snapshot in Fig. 8 (top left) by 60 degrees.

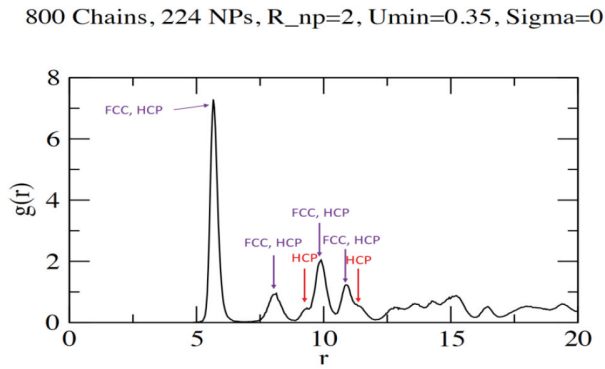

Figure 7. A graph that provides the pair-pair correlation function of NPs in a system of 800 Chains, 224 NPs, 0.35 Umin, and a grafting density of 0.5. Peaks that are characteristic of face-centered cubic (FCC) and hexagonal close packed (HCP) structures are notated.

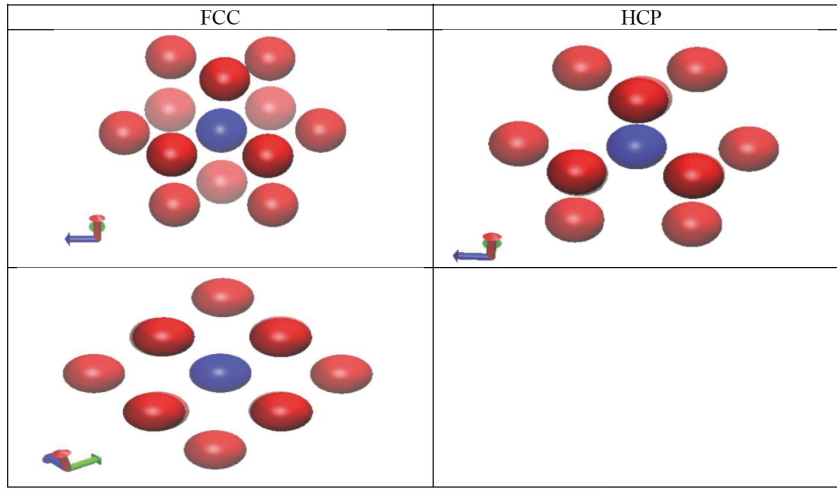

Figure 8. Snapshots taken from a system of 800 chains, 224 NPs, 0.35 $|U_{min}|$, and a grafting density of 0.5

The fact that order was observed is highly surprising. This is a preliminary study into such systems, and not many arguments exist as to why this occurs. One that can be made is due to the conformational entropy of the polymer chains. As the NPs are absorbed, some chains are compressed quite a bit as shown in Fig. 9. This reduction of entropy is not preferred by the chains, therefore there could be some counter-active force upward along the z-axis. This force is in competition with the attractive potential which is orientated downwards. There appears to be some optimal balance between these two forces that leads to the surprising order that we have observed.

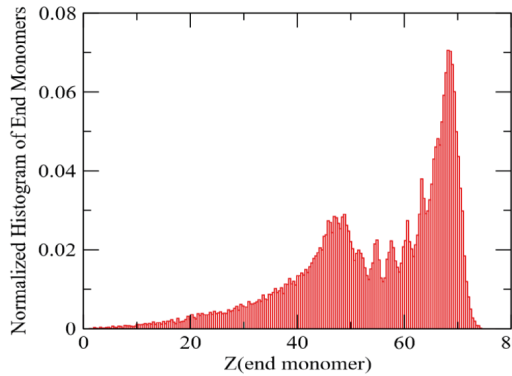

Figure 9. Normalized histogram of end-to-end distances of the polymer chains NPs in a system of 800 Chains, 224 NPs, 0.35 Umin, and a grafting density of 0.5.

Conclusions

This paper presents a course-grained implicit-solvent model of many NPs at the interface of a polymer brush. A systematic study of such model was then preformed. In this study, the fraction of NPs absorbed into the brush was highly correlated with $|U_{min}|$; as $|U_{min}|$ was increased, so was the fraction absorbed. This fraction begins to receive a non-trivial increase at values of $|U_{min}|$ as low as 0.1. There also exists a strong dependence between $|U_{min}|$ and the preferred location of the NPs in the polymer brush. As $|U_{min}|$is increased, the average height of the NPs begins to decrease. The average height can only be decreased until it saturates at a minimum value prescribed by the polymer brush. The NPs cannot penetrate further than this minimum value regardless of the value of $|U_{min}|$. The minimum value is directly related to the grafting density of the brush.

One striking phenomenon noted in this study was the formation of superstructures. For the case of a polymer brush with grafting density of 0.5 and 800 chains, a range of superstructures were visible for values of $|U_{min}| \approx 0.3$. These superstructures were formed in an undefined orientation and consisted of both FCC and HCP unit cells. Due to the aggregation of NPs into one portion of the brush, there is a clear compression of the polymer chains leading to a reduction in conformational entropy. This reduction could be a leading factor in the advent of these superstructures.

This was a computational preliminary study into such a system; as such it is meant to be a starting point for other studies into this interesting phenomenon. Our systematic numerical study showcases the self-assembly of superstructures for a range of NP-polymer interactions. It is with great hope that other researchers will be able to use the qualitative and quantitative information of this study to probe into such systems experimentally.

Acknowledgements

This research would not be possible without the REU program at the University of Memphis funded by the NSF. I extend my greatest thanks to the NSF for this opportunity. All simulations were done on the HPC at the University of Memphis. I would like to thank Eric Spangler for his continued help with computing, and my supervisor Dr. Mohamed Laradji for helping me and allowing me to work through such a project. Thanks also go to the staff of *Quaesitum* for their continued work on this journal, as they provide a much-needed platform for the research conducted by undergraduate students here at the University of Memphis.

References

1. Jaeup U. Kim and Mark W. Matsen, "Repulsion Exerted on a Spherical Particle by a Polymer Brush", Macromolecules, 41, 1, 246–252, (2007). doi: https://doi.org/10.1021/ma071906t

2. Dikran Kesal, Stephanie Christau, Patrick Krause, Tim Möller, and Regine Von Klitzing, "Uptake of pH-Sensitive Gold. Nanoparticles in Strong Polyelectrolyte Brushes", Polymers (Basel). (2016) doi: 10.3390/polym8040134.

3. Eric J. Spangler, P. B. Sunil Kumar, and Mohamed Laradji, "Stability of membrane-induced self-assemblies of spherical nanoparticles". Soft Matter. doi: https://doi.org/10.1039/C8SM00537K

4. Eric J. Spangler and Mohamed Laradji, "Spatial arrangements of spherical nanoparticles on lipid vesicles", J. Chem. Phys. 154, 244902 (2021). doi: https://doi.org/10.1063/5.0054875

5. Shengfeng Cheng, Mark J. Stevens, and Gary S. Grest, "Ordering nanoparticles with polymer brushes", J. Chem. Phys. 147, 224901 (2017) doi: https://doi.org/10.1063/1.5006048

6. Michael R. Bockstaller, Yonit Lapetnikov, Shlomo Margel, and Edwin L. Thomas, "Size-Selective Organization of Enthalpic Compatibilized Nanocrystals in Ternary Block Copolymer/Particle Mixtures". doi: https://doi.org/10.1021/ja034523t

7. Joel D. Revalee, Mohamed Laradji, and P. B. Sunil Kumar, "Implicit-solvent mesoscale model based on soft-core potentials for self-assembled lipid membranes", J. Chem. Phys. 128, 035102 (2008) doi: https://doi.org/10.1063/1.2825300

8. Mohamed Laradji et al 2016 J. Phys. D: Appl. Phys. 49 293001

9. Eric J. Spangler, Alexander D. Olinger, P. B. Sunil Kumar, and Mohamed Laradji, "Binding, unbinding and aggregation of crescent-shaped nanoparticles on nanoscale tubular membranes", Soft Matter, 2021,17, 1016-1027, doi: https://doi.org/10.1039/D0SM01642J

10. William C. Swope, Hans C. Andersen, Peter H. Berens, and Kent R. Wilson, "A computer simulation method for the calculation of equilibrium constants for the formation of physical clusters of molecules: Application to small water clusters", J. Chem. Phys. 76, 637-649 (1982) doi: https://doi.org/10.1063/1.442716